Gremlin-mediated BMP antagonism induces the epithelial-mesenchymal feedback signaling controlling metanephric kidney and limb organogenesis

Odyssé Michos[1,2], Lia Panman[2], Kristina Vintersten[3,*], Konstantin Beier[4], Rolf Zeller[1] and Aimée Zuniga[1,†]

[1]Developmental Genetics, Dept. of Clinical-Biological Sciences (DKBW), University of Basel Medical School, c/o Anatomy Institute, Pestalozzistrasse 20, CH-4056 Basel, Switzerland
[2]Department of Developmental Biology, Utrecht University, Padualaan 8, NL-3584CH Utrecht, The Netherlands
[3]Transgenic Service, EMBL, Meyerhofstrasse 1, D-69117 Heidelberg, Germany
[4]Department of Histology, Anatomy Institute, Pestalozzistrasse 20, CH-4056 Basel, Switzerland
*Present address: Mount Sinai Hospital, Samuel Lunenfeld Research Institute, Stem Cell Mutagenesis Laboratory, 600 University Avenue, Toronto, Ontario M5G1X5, Canada
†Author for correspondence (e-mail: aimee.zuniga@unibas.ch)

Accepted 5 May 2004

Development 131, 3401-3410
Published by The Company of Biologists 2004
doi:10.1242/dev.01251

Summary

Epithelial-mesenchymal feedback signaling is the key to diverse organogenetic processes such as limb bud development and branching morphogenesis in kidney and lung rudiments. This study establishes that the BMP antagonist gremlin (*Grem1*) is essential to initiate these epithelial-mesenchymal signaling interactions during limb and metanephric kidney organogenesis. A *Grem1* null mutation in the mouse generated by gene targeting causes neonatal lethality because of the lack of kidneys and lung septation defects. In early limb buds, mesenchymal *Grem1* is required to establish a functional apical ectodermal ridge and the epithelial-mesenchymal feedback signaling that propagates the sonic hedgehog morphogen. Furthermore, *Grem1*-mediated BMP antagonism is essential to induce metanephric kidney development as initiation of ureter growth, branching and establishment of RET/GDNF feedback signaling are disrupted in *Grem1*-deficient embryos. As a consequence, the metanephric mesenchyme is eliminated by apoptosis, in the same way as the core mesenchymal cells of the limb bud.

Key words: BMP antagonism, *Grem1*, Gremlin, Kidney, Limb bud, Mouse, Organogenesis

Introduction

Vertebrate organogenesis is orchestrated by signaling centers with organizer properties that coordinate cell proliferation and survival with cell specification and differentiation. Signaling by cells with special organizer properties instructs undetermined neighboring cells with respect to their fate and differentiation potential. Such reciprocal epithelial-mesenchymal signaling interactions control growth and patterning of morphologically very diverse embryonic structures, including limbs, kidneys and lungs in vertebrates. In particular, the molecular epithelial-mesenchymal signaling interactions regulating branching morphogenesis have recently provided novel insights into how tissues are organized in space as organogenesis proceeds (Affolter et al., 2003). Two models of paradigmatic value to study morphogenetic epithelial-mesenchymal signaling interactions in vertebrate embryos are the limb bud (Tickle, 2003) and branching morphogenesis of the ureter during kidney organogenesis (Vainio and Lin, 2002). In particular, two main signaling centers control limb bud development: the sonic hedgehog (*Shh*)-expressing polarizing region, which is located in the posterior limb bud mesenchyme; and the apical ectodermal ridge (AER), a differentiated columnar epithelium expressing different types of signaling peptides. SHH signaling by the polarizing region controls patterning of distal limb structures and its expression is regulated by fibroblast growth factor (FGF) signaling from the AER (SHH/FGF feedback loop) (Panman and Zeller, 2003). Genetic analysis in the mouse indicates that the AER expressed FGFs, such as FGF8 and FGF4, cooperate to activate and positively regulate *Shh* expression in the posterior limb bud mesenchyme (Lewandoski et al., 2000; Moon and Capecchi, 2000; Sun et al., 2002). The bone morphogenetic protein (BMP) antagonist gremlin (*Grem1*) (Hsu et al., 1998) is a cystein knot protein belonging to the CAN family that antagonizes preferentially BMP2 and BMP4 (Avsian-Kretchmer and Hsueh, 2003). *Grem1* is expressed by a subset of SHH responsive mesenchymal cells and has been implicated in transducing the SHH signal to the posterior AER. This results in activation of *Fgf4* expression and establishment of the SHH/FGF4 feedback loop (Capdevila et al., 1999; Zuniga et al., 1999).

In addition to the limb bud, *Grem1* is expressed by a variety of embryonic structures including lung (Lu et al., 2001; Shi et al., 2001) and kidney rudiments (this study). Development of the definitive metanephric kidney is initiated by formation and growth of the ureteric bud. As the ureteric bud invades the metanephric mesenchyme, it induces condensation and nephrogenesis through reciprocal interactions (Saxén, 1987). Genetic analysis in the mouse shows that the *Wt1* and *Pax2* transcription factors (Kreidberg et al., 1993; Torres et al., 1995) control the induction of metanephric development. By contrast, the extracellular signals that trigger ureteric bud formation in the posterior part of the Wolffian duct and initiate ureter growth and branching have so far remained largely elusive. The tips of the invading ureter express the tyrosine kinase receptor RET (Pachnis et al., 1993; Towers et al., 1998), whereas RET ligand GNDF is expressed in the condensing metanephric mesenchyme (Hellmich et al., 1996; Towers et al., 1998). Genetic analysis has established that the epithelial-mesenchymal signaling interactions mediated by RET and GNDF are essential for metanephric development (Vainio and Lin, 2002). BMP signaling has also been implicated in metanephric development as potential regulator of ureter growth, branching and nephrogenesis (Dudley et al., 1995; Luo et al., 1995; Martinez and Bertram, 2003; Miyazaki et al., 2000; Raatikainen-Ahokas et al., 2000). In particular *Bmp4*, which is expressed by the mesenchyme surrounding the Wolffian duct and ureter stalk seems to fulfill a dual function during early metanephric development. Heterozygous *Bmp4* mutant mouse embryos display a variable kidney phenotype characterized by defects in ureteric epithelium growth and induction of ectopic ureter branching (Miyazaki et al., 2000; Raatikainen-Ahokas et al., 2000). These studies have also provided evidence that BMP signaling regulates ureteric bud initiation and branching. An involvement of BMP antagonism has been postulated, but the relevant antagonist(s) remained to be identified (Miyazaki et al., 2000). To study the essential functions of the BMP antagonist *Grem1*, we have deleted the *Grem1* open reading frame (ORF) by homologous recombination in mouse embryonic stem (ES) cells. We report that *Grem1*-deficient mice die shortly after birth because of disruption of kidney and lung organogenesis. During limb bud development, *Grem1* is required for survival of core mesenchymal cells and to establish a functional AER expressing different types of signals, which regulate *Shh* expression and progression of limb bud morphogenesis. During kidney organogenesis, *Grem1* is required to initiate ureter growth and branching that in turn induces metanephric nephrogenesis. Together, these results reveal a common and essential role of *Grem1*-mediated BMP antagonism in initiating dynamic epithelial-mesenchymal signaling.

Materials and methods

Generation of the *Gre*$^{\Delta ORF}$ null allele

We generated the targeting vector using a 4.8 kb *Nde*I-*Xba*I and a 5.6 kb *Nsi*I-*Nsi*I *Gre* genomic fragment isolated from a 129/SvJ Lambda FIXII library (Stratagene). We inserted an IRES-*lacZ* gene and a PGK-*Neo*^{R} cassette flanked by two *lox*P sites in the same transcriptional orientation as the *Grem1* gene. R1 ES-cells were electroporated with the *Not*I linearized targeting vector and screened by genomic Southern with an *Nsi*I-*Eco*RI probe mapping outside the 3′ homology arm (Fig. 1A). Thirty-five homologous recombined ES-cell clones were obtained at a frequency of 10.8%. Correct recombination resulting in the deletion of the entire 552 base *Grem1* ORF encoded by exon 2 and of 132 bases of the 3′ UTR was confirmed by extensive Southern blot and PCR analysis. ES cells carrying the *Gre*$^{\Delta ORF}$ null allele were injected into C57BL/6 blastocysts and, following germline transmission, the mice were maintained in mixed B6;129S and CD1 backgrounds. PCR genotyping was used for all subsequent studies to allow specific detection of both the wild-type and *Gre*$^{\Delta ORF}$ alleles. The floxed PGK-*neo*^{R} gene was removed by crossing *Gre*$^{\Delta ORF}$ heterozygous mice with the *Cre* deleter strain. The sequence of the murine *Grem1* locus was obtained from the UCSC Genome Bioinformatics Website (http://genome.ucsc.edu/) and analyzed using the DNA Strider 1.3*TM* program. The *Gre*$^{\Delta ORF}$ mutation was crossed into 129S3/SvImJ, C57BL/6 and CD1 strains as the penetrance of the kidney phenotype depends on genetic background. In the 129S and CD1 backgrounds, the kidney phenotype is fully penetrant (Fig. 2B).

Molecular and morphological analysis of embryos and newborn mice

Embryos and newborn mice were PCR genotyped and accurately staged by determining their somite numbers. Whole-mount and section RNA in situ hybridization were performed as previously described (Dono et al., 1998; Zuniga et al., 1999) using digoxigenin-UTP-labeled anti-sense riboprobes. Apoptotic cells were detected in situ by incorporating fluorescein-dUTP into fragmented DNA using terminal transferase (Roche Diagnostics). For histological analysis, sections were cut from formalin-fixed and paraffin-embedded material and stained with Hematoxylin and Eosin using standard protocols. For scanning electron microscopy (SEM), embryos were fixed in 1% gluteraldehyde (Sigma) for 1 hour at 4°C and processed for SEM.

In vitro grafting and culturing of mouse limb buds (trunk cultures)

Mouse forelimb buds were cultured and grafted as described (Zuniga et al., 1999) with the following modifications. Trunks with attached forelimb buds were isolated from either wild type, heterozygous or *Grem1*-deficient embryos. Embryos were staged by counting somites and genotyped by PCR. Spherical cell aggregates were grafted into the forelimb buds and trunks and were cultured for 15 hours in serum-free medium in 6.5% CO_2 at 37°C. The culture medium was prepared by supplementing high glucose DMEM (GIBCO BRL) medium, with L-glutamine, penicillin/streptomycin, non-essential amino acids, sodium pyruvate, D-glucose, L-ascorbic acid, lactic acid, d-biotin, vitamin B12 and PABA. QT6 fibroblast cells expressing *Shh* and *Grem1* under control of the CMV promoter were prepared using standard calcium phosphate transfection (Zuniga et al., 1999). One day after transfection, spherical cell aggregates were prepared by plating cells at high density on bacterial plates. The following day, cells were treated with mitomycin C for 1 hour to block proliferation. After washing the cell aggregates extensively, they were grafted into recipient limb buds (a detailed protocol for media preparation, limb bud grafting and culturing is available upon request).

Results

Disruption of the *Gremlin 1* ORF results in multiple organ defects causing neonatal lethality

The second exon of the *Grem1* gene, which encodes the complete ORF, was inactivated by homologous recombination in R1 ES-cells as shown in Fig. 1A. The complete *Grem1* coding exon 2 was deleted and replaced by a *lacZ* marker and a *Neomycin* resistance (*Neo*^{R}) gene flanked by two *loxP* sites. Correctly targeted ES-cell clones were identified by Southern blot screening (Fig. 1B,C) and two independent clones were used to generate *Gre*$^{\Delta ORF}$ mice (Fig. 1D). Heterozygous mice of both strains appear normal and the distribution of *Grem1* and *Gre-lacZ* fusion transcripts (Fig. 1A) are identical (Fig. 1E). By contrast, *Gre*$^{\Delta ORF}$ homozygous newborn mice display

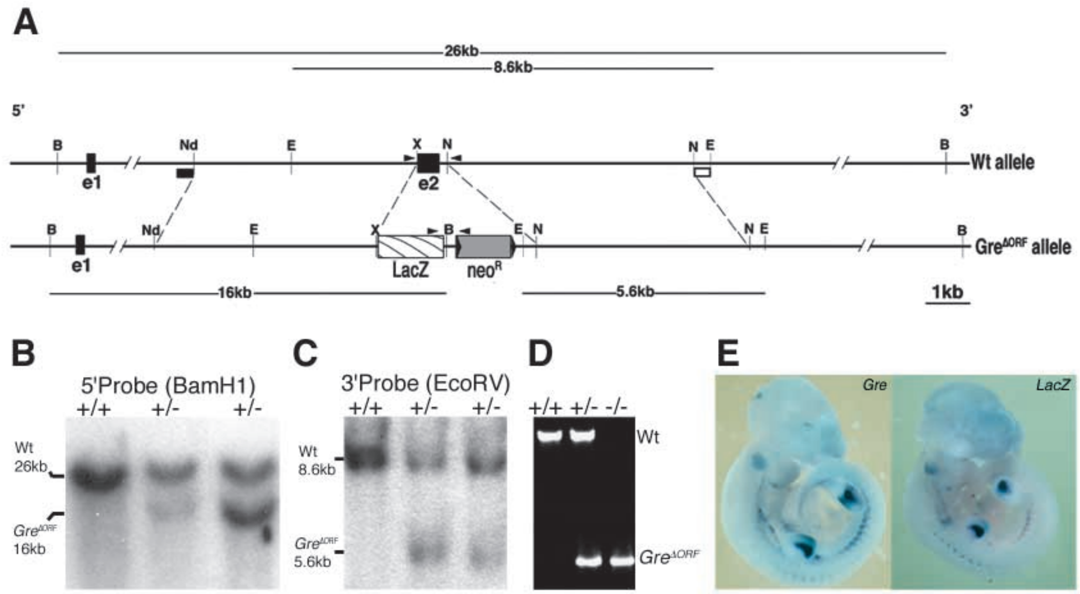

Fig. 1. Generation of a *Grem1* loss-of function mutation by gene targeting. (A) The *Gre*$^{\Delta ORF}$ loss-of-function allele was generated by homologous recombination in ES cells. The entire ORF encoded by exon 2 (e2) was replaced with an IRES-*lacZ* gene and the *Neo*^{R} cassette (flanked by *lox*P sites indicated by black triangles). Exon 1 (e1) is non-coding and located 8.5 kb upstream of exon 2 (UCSC). The 5′ and 3′ genomic probes used to screen ES-cell clones by Southern blotting are indicated by black and white boxes, respectively. Thin black lines indicate the sizes of the expected genomic bands detected by these probes. Arrowheads indicate the primers used to detect both wild-type (Wt) and mutant (*Gre*$^{\Delta ORF}$) alleles. The relevant restriction enzyme sites are indicated as follows: B, *Bam*HI; E, *Eco*RV; N, *Nsi*I; Nd, *Nde*I; X, *Xba*I. (B,C) Analysis of wild-type (+/+) and correctly targeted heterozygous (+/–) ES-cell clones by Southern blotting using 5′ and 3′ genomic probes. (D) PCR genotyping of embryos of F2 littermate embryos. (E) Whole-mount in situ hybridization using *Gre*$^{\Delta ORF/+}$ embryos at embryonic day 11.0 reveals the identical distribution of *Grem1* and *lacZ* transcripts.

limb defects (Fig. 2G-J) and die shortly after birth. Autopsy at birth reveals that *Gre*$^{\Delta ORF}$ homozygous newborn mice lack metanephric kidneys and ureters (compare Fig. 2A with 2B; data not shown), whereas the remainder of the urogenital system appears normal. In addition, newborn *Grem1* deficient mice display respiratory problems (dyspnoe and cyanosis) that probably contributes significantly to their early death. Indeed, septation of the lung airway epithelium is affected as numbers of differentiated alveoli are reduced in *Grem1*-deficient newborn mice (compare Fig. 2C with 2D). Furthermore, the airway epithelium remains multi-layered in comparison with wild-type embryos (compare Fig. 2E with 2F). Cre recombinase-mediated removal of the *Neo*^{R} gene does not alter the phenotypes, confirming that they are due to the *Grem1* deficiency (data not shown). As initial analysis indicated that the lung septation defects arise only during advanced lung organogenesis, the present study focuses on analyzing the early pattern defects that disrupt limb bud and kidney organogenesis.

The limb phenotypes observed in *Grem1*-deficient mice correspond to a strong and fully penetrant *ld* limb phenotype (Fig. 2G-J). The zeugopods of *Grem1*-deficient newborn mice are differentially affected as ulna and radius fuse during onset of ossification, while only one skeletal element forms in hind limbs (arrows, Fig. 2G-J). The autopods are severely truncated because of metacarpal fusions (arrowheads, Fig. 2H,J), reductions in digit numbers and loss of posterior identities together with soft tissue webbing (Fig. 2H,J; data not shown).

Mesenchymal *Gremlin 1*-mediated BMP antagonism is required for proper AER formation and epithelial-mesenchymal signaling in limb buds

During limb bud morphogenesis, the number of *Shh*-expressing cells and transcript levels increase progressively in wild-type embryos (Fig. 3A) (Riddle et al., 1993). By contrast, the *Shh* expression domain remains small and levels stay low in limb buds of *Gre*$^{\Delta ORF}$ homozygous embryos (Fig. 3A; data not shown). This failure to propagate SHH signaling has been attributed to the disruption of the SHH/FGF4 feedback loop (Haramis et al., 1995; Khokha et al., 2003; Zuniga et al., 1999). However, analysis of *Gre*$^{\Delta ORF}$ homozygous embryos reveals a general disruption of AER morphology and function (Figs 3, 4). Activation of *Fgf8* in the limb bud ectoderm and thereby initiation of AER formation occur normally in *Grem1*-deficient limb buds (Fig. 3B, E9.5). However, the *Fgf8*-expressing AER cells remain more spread out along the dorsoventral ectoderm, revealing the early disruption of AER morphology in *Grem1*-deficient limb buds (Fig. 3B, E9.75). As development proceeds, *Fgf8*-expressing cells become restricted to the apex, but the domain remains patchy in mutant limb buds (Fig. 5E,G; data not shown), owing to the defects in AER morphology (Fig. 4E,F). In addition, FGF signaling by the posterior AER (Martin, 1998) is completely disrupted as neither *Fgf4* nor *Fgf9* nor *Fgf17* is activated in *Grem1*-deficient limb buds (Fig. 3C and data not shown).

This general alteration of AER morphology and function could be a direct consequence of enhanced BMP signaling as it has been shown that BMPs, although required to induce the

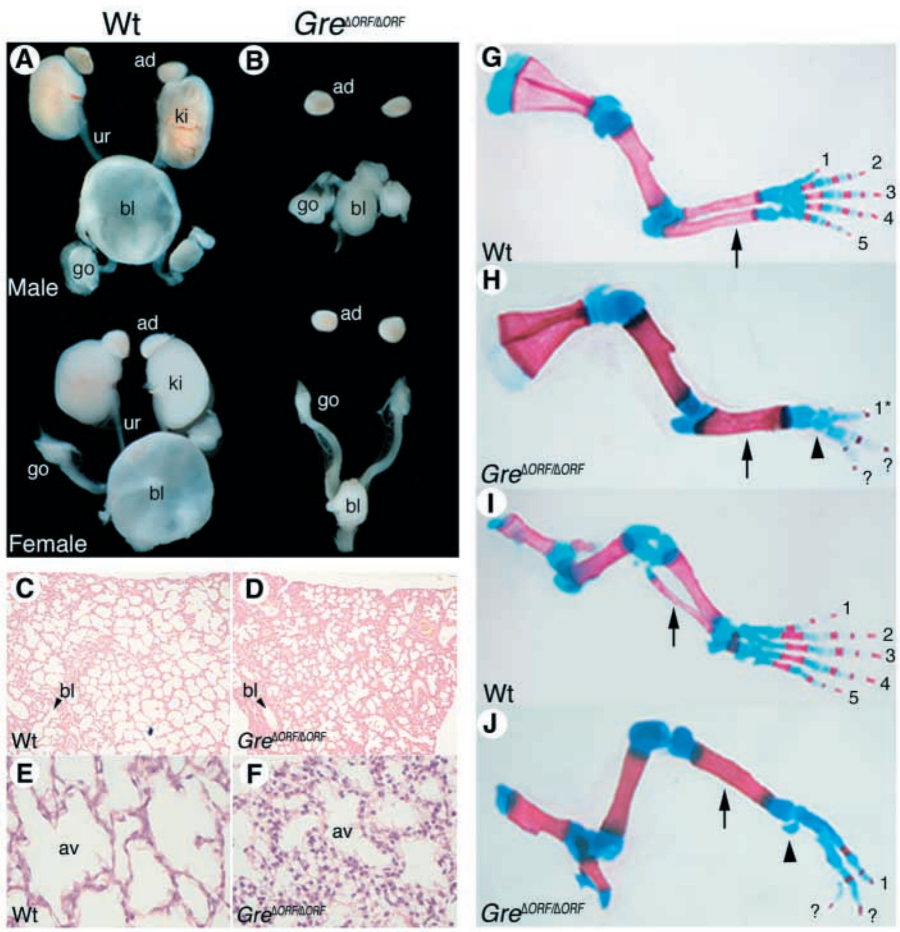

Fig. 2. The *Grem1* deficiency causes neonatal lethality because of complete bilateral renal agenesis and lung defects in combination with distal limb defects. (A,B) Urogenital defects in $Gre^{\Delta ORF}$ homozygous newborn mice. Mutant mice display complete bilateral agenesis of the kidney (ki) and ureter (ur). Note that gonads (go) and adrenal glands (ad) form correctly, while the bladder (bl) is not filled in mutant mice. (C-F) Lung defects in newborn *Grem1*-deficient mice. (C,D) Transversal histological sections through the lung of newborn wild-type mouse (C) and *Grem1*-deficient mouse (D) at the level of the heart. (E,F) High-magnification views of a longitudinal section through the lungs of a wild-type (E) and a *Grem1*-deficient (F) newborn mice. av, alveoli; bl, bronchiole. (G-J) Limb skeletal abnormalities in $Gre^{\Delta ORF}$ homozygous newborn mice; (G,H) forelimbs, (I,J) hindlimbs. Arrows indicate the zeugopod; arrowheads indicate metacarpal bones. Digit numbers are reduced and identities lost in $Gre^{\Delta ORF/\Delta ORF}$ limbs. Asterisk indicates a fused digit 1; question marks indicate posterior digits with unclear identities.

AER, interfere with formation of the mature and fully functional AER (Pizette and Niswander, 1999; Pizette et al., 2001). *Msx1* and *Msx2* are targets of BMP signaling in the limb bud and can be used as in situ indicators of enhanced and/or ectopic BMP signaling (Pizette et al., 2001). *Msx1* and *Msx2* are activated normally (Fig. 4A and data not shown), but subsequently ectopically expressed in the distal to anterior sub-AER limb bud mesenchyme of *Grem1*-deficient embryos (Fig. 4B; data not shown). This upregulation is indicative of enhanced BMP signaling in the sub-AER mesenchyme due to lack of *Grem1*-mediated BMP antagonism. Indeed, expression of both *Bmp4* and *Bmp7* is maintained in the limb bud mesenchyme of *Grem1*-deficient embryos, while *Bmp2* is reduced from early stages onwards (Fig. 4C; data not shown). Therefore, overall *Bmp* transcript levels appear unaffected in the sub-AER mesenchyme, where BMP signaling is enhanced due to lack of *Grem1* function (compare Fig. 4B with 4C). Furthermore, *Bmp* expression is activated in the mutant AER, but not maintained during progression of limb bud morphogenesis (Fig. 4D; data not shown). Morphological analysis by scanning electron microscopy reveals that the apical ectodermal cells of $Gre^{\Delta ORF}$ homozygous limb buds fail to adopt the characteristic ridge-like morphology (Fig. 4E), although AER-type cells are present (Fig. 4F). Taken together, these results establish that induction of *Fgf8*-expressing AER cells occurs normally, while formation of a morphologically distinct and functional AER depends critically on *Grem1*-mediated antagonism of BMP signaling in the distal/sub-AER mesenchyme.

Particularly *Bmp2* has been considered a direct transcriptional target of SHH signaling in the mesenchyme (Drossopoulou et al., 2000). Therefore, reduced *Bmp2* expression could be a consequence of reduced SHH signaling and thus secondary to disrupting *Grem1*. However, posterior grafts of *Shh*-expressing fibroblasts, which are capable of rescuing gene expression (Zuniga et al., 1999), fail to upregulate *Bmp2* expression in limb buds of $Gre^{\Delta ORF}$ homozygous embryos (Fig. 5A,B). By contrast, grafts of *Grem1*-expressing fibroblasts enhance mesenchymal *Bmp2* transcription and restore *Bmp2* expression in the AER of mutant limb buds (Fig. 5C,D). Similarly, *Grem1* (Fig. 5G,H) but not *Shh* grafts (Fig. 5E,F) restore *Fgf8*, *Fgf4* (Zuniga et al., 1999) and *Fgf9* (data not shown) expression in the AER of mutant limb buds. These results establish that mesenchymal *Grem1* modulates *Bmp2* and *Fgf8* expression positively and is required for activation of FGF genes in the posterior AER.

Gremlin 1 is essential for metanephric kidney organogenesis

The bilateral renal agenesis in $Gre^{\Delta ORF}$ homozygous newborn mice in the context of an otherwise normal urogenital system (Fig. 2B) indicates an unexpected essential role of *Grem1* during metanephric kidney organogenesis. Metanephric kidney development is initiated by invasion and induction of the

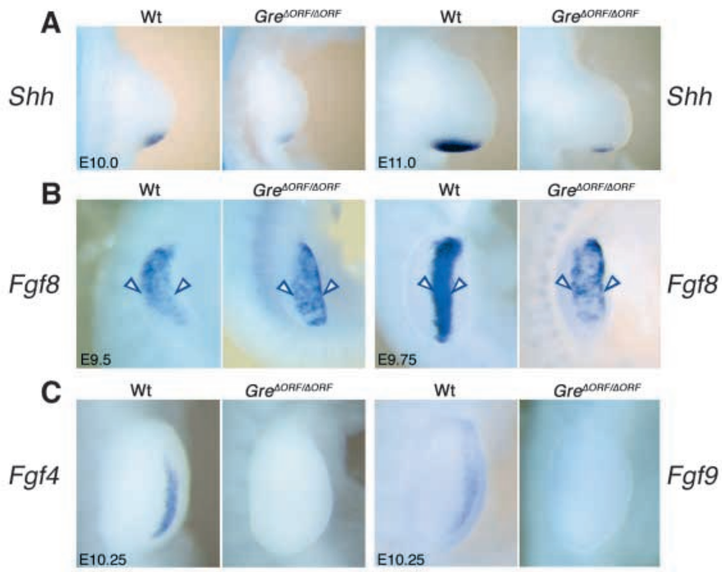

Fig. 3. *Grem1* is required for propagation of *Shh* in the limb bud mesenchyme and for FGF gene expression in the AER. (A) *Shh* expression in wild-type and *Grem1* (*Gre*$^{\Delta ORF/\Delta ORF}$)-deficient limb buds during E10.0 and E11.0. The *Shh* expression domain is activated but not propagated in mutant limb buds. Posterior is towards the bottom and distal towards the right. (B) Expression of *Fgf8* is activated normally (E9.5), but the domain remains broader and patchy in mutant limb buds (arrowheads, E9.75). (C) Neither *Fgf4* nor *Fgf9* expression is activated in mutant limb buds (E10.25). All limb buds shown are fore limb buds. In B,C, posterior is towards the bottom and dorsal towards the left.

metanephric mesenchyme by the ureter between embryonic days 10.5 to 11.0 in mouse embryos (Vainio and Lin, 2002). *Grem1* is initially expressed by the intermediate mesenchyme (Pearce et al., 1999) and from about embryonic day 9.5 onwards by the Wolffian duct and mesonephric tubules (Fig. 6A and data not shown). During onset of metanephric development, *Grem1* is rapidly downregulated and restricted posteriorly in the Wolffian duct (Fig. 6B; data not shown). At this stage, *Grem1* is expressed locally in the condensing metanephric mesenchyme, which surrounds the ureteric bud (Fig. 6C). The *Pax2* transcription factor is essential for urogenital development and acts upstream of the signal(s) initiating metanephric development (Torres et al., 1995). During ureteric bud formation, *Pax2* expression is not affected in *Gre*$^{\Delta ORF}$ homozygous embryos (data not shown). By contrast, invasion of the metanephric mesenchyme by the ureter and upregulation of *Pax2* expression in the induced mesenchyme fail to occur in *Grem1* deficient embryos (Fig. 6D). The failure to induce metanephric development becomes more apparent as development progresses. *Pax2* expression is lost from the mutant metanephric mesenchyme by embryonic day 12.5, while nephrogenesis progresses in wild-type embryos (Fig. 6E). In addition, *Bmp2*, *Bmp7* (Fig. 6F,G) and *Wnt4* transcripts (data not shown) are absent from the mutant metanephric mesenchyme. These results are indicative of a possible failure to induce condensation of the metanephric mesenchyme.

The failure to induce metanephric organogenesis is due to a complete disruption of ureter growth and branching

The tyrosine kinase receptor RET and its ligand GDNF are expressed by the ureter epithelium and mesenchyme, respectively (Fig. 7A) (Hellmich et al., 1996; Pachnis et al., 1993; Towers et al., 1998). In *Gre*$^{\Delta ORF}$ homozygous embryos, both *Ret* and *Gdnf* expression are activated and the ureteric bud

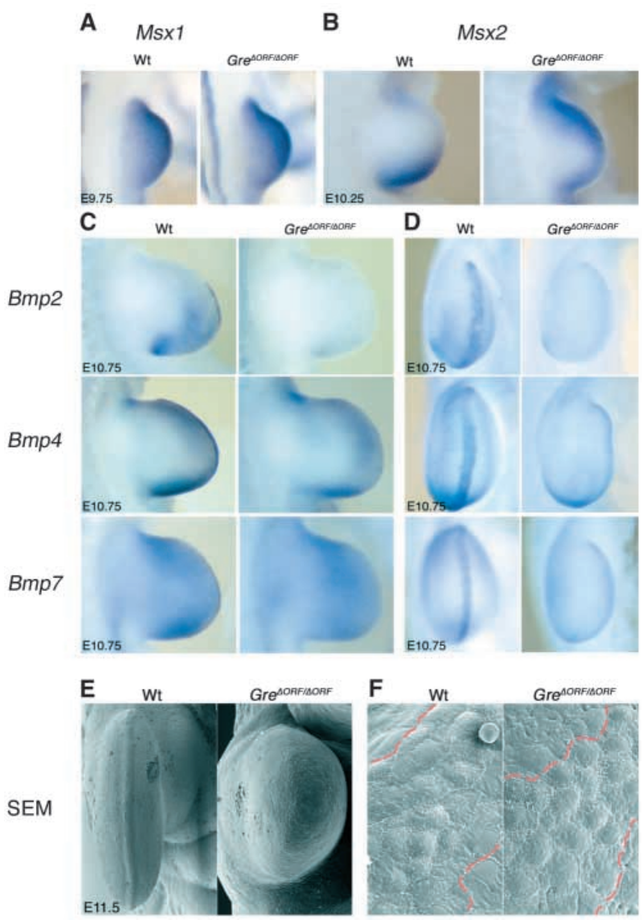

Fig. 4. BMP signaling and expression in *Grem1*-deficient limb buds. (A) Expression of the BMP target *Msx1* during early limb bud development (E9.75). (B) Expression of the BMP target *Msx2* during limb bud development (E10.25). Note ectopic *Msx2* expression in the distal to anterior limb bud mesenchyme of *Grem1* (*Gre*$^{\Delta ORF/\Delta ORF}$)-deficient embryos, which is indicative of enhanced BMP signaling. (C) Expression of *Bmp2*, *Bmp4* and *Bmp7* in the limb bud mesenchyme (E10.75). Mesenchymal *Bmp2* expression is significantly reduced at this stage in *Grem1*-deficient limb buds, while *Bmp4* and *Bmp7* are maintained at normal levels. (D) *Bmp2*, *Bmp4* and *Bmp7* expression in the AER of wild-type and *Grem1* mutant forelimb buds (E10.75). Expression of all three (*Bmp2*, *Bmp4* and *Bmp7*) is lacking from the AER of mutant limb buds. (E) Scanning electronic microscopy analysis of wild-type and *Grem1*-deficient forelimb buds (E11.5). Note that the AER of mutant limb buds is poorly differentiated and the anteroposterior limb bud axis is shortened in comparison with the wild type. In D,E, posterior is towards the bottom and dorsal is towards the left. (F) High-power SEM revealing the morphology of AER-type ectodermal cells (outlined in red).

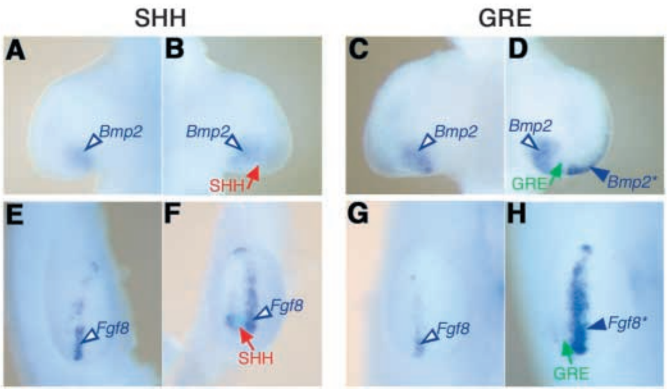

Fig. 5. *Grem1*, but not SHH, rescues *Fgf8* and *Bmp2* expression in the AER of *Gre*$^{\Delta ORF/\Delta ORF}$ limb buds. All grafted limb buds are forelimb buds (E10.5) of *Grem1* mutant embryos. Limb buds either received *Shh* (red arrow) or *Grem1* (green arrow)-expressing cell aggregates and were cultured for 15 hours prior to analysis. White arrowheads indicate the endogenous expression domains; blue arrowheads and asterisks indicate the induced expression. (A) *Bmp2* expression in a non-grafted control limb bud of a mutant embryo. (B) Posterior grafts of *Shh*-expressing cell aggregates fail to rescue *Bmp2* expression. (C,D) Posterior grafts of *Grem1*-expressing cells induce *Bmp2* expression in the AER (D), while no *Bmp2* transcripts are detected in the AER of non-grafted mutant limb buds (C). Note also the enhancement of mesenchymal *Bmp2* expression (D). (E,F) Posterior grafts of *Shh*-expressing cells do not rescue *Fgf8* expression in the AER (F) in comparison with a non-grafted mutant limb buds (E). (G,H) Posterior grafts of *Grem1*-expressing cells induce upregulation of *Fgf8* expression in the AER (H) in comparison with endogenous *Fgf8* expression in non-grafted mutant limb buds (G). (A-D) Dorsal views with posterior towards the bottom and distal towards the right; (E-H) posterior is towards the bottom and dorsal towards the left.

forms (Fig. 7B; data not shown), possibly as a consequence of activating RET/GNDF signaling. However initiation of ureter growth (arrow, Fig. 7A) and *Gdnf* upregulation are completely blocked in *Grem1*-deficient embryos (Fig. 7B, compare with Fig. 7A). The ureter branches (arrowheads, Fig. 7C) as it invades the metanephric mesenchyme. The branching tips of the wild-type ureter express high levels of *Ret* and *Gdnf* is upregulated in the surrounding, condensing mesenchyme (Fig. 7E). By contrast, the ureteric bud does not branch in *Grem1*-deficient embryos (Fig. 7D) and mesenchymal *Gdnf* expression is rapidly lost, despite continued *Ret* expression by the arrested epithelium (Fig. 7D,F).

Gremlin 1 mediated BMP antagonism promotes survival of mesenchymal cells

To understand how the molecular alterations give rise to the distal limb defects and result in elimination of the metanephric kidney, potential effects on programmed cell death were assayed. Massive cell death is observed in the core mesenchyme of *Grem1*-deficient limb buds by embryonic day 11.0 (Fig. 8A). However, the superficial dorsal and ventral limb bud mesenchymal cells normally expressing *Grem1* (Merino et al., 1999) survive in limb buds of *Gre*$^{\Delta ORF}$ homozygous embryos as indicated by the continued presence of *lacZ*-expressing cells (Fig. 8B). Similarly, *lacZ*-expressing cells remain in the Wolffian duct and mesenchyme of *Grem1*-deficient embryos (data not shown) in spite of massive aberrant cell death at embryonic day 11.5 (Fig. 8C). Analysis of parallel sections shows that the metanephric mesenchyme, which expresses *Pax2* (Fig. 8D), is eliminated by apoptosis.

Discussion

We show that inactivation of *Grem1* in the mouse causes a limb phenotype in combination with complete renal agenesis and lung airway defects. In particular, the gross morphological appearance of the limb and kidney phenotypes is strikingly

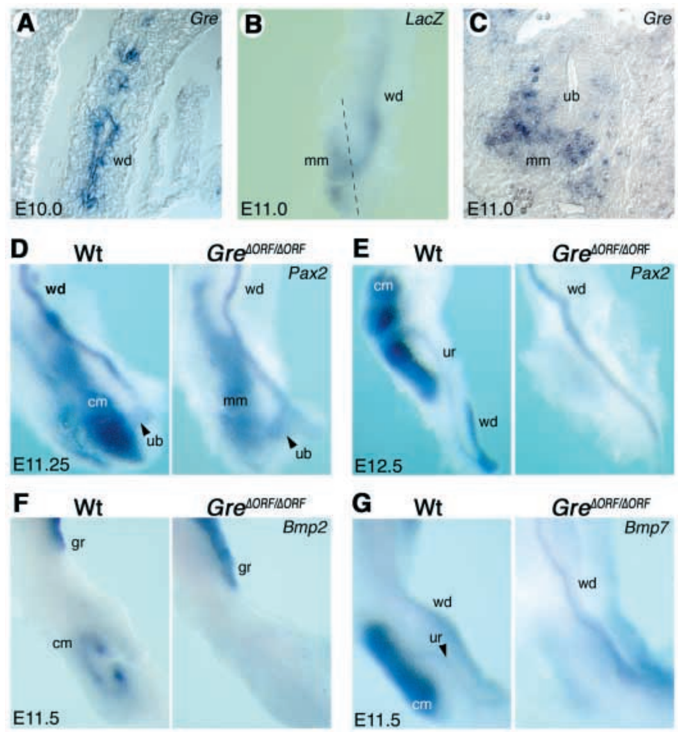

Fig. 6. Disruption of metanephric kidney morphogenesis. (A-C) Distribution of *Grem1* transcripts during kidney morphogenesis. (A) *Grem1* expression in the Wolffian duct and mesonephric tubules during E10.0. (B) Distribution of *Grem1* transcripts during initiation of metanephric development (E11.0). The distribution of *lacZ* transcripts in a *Gre*$^{\Delta ORF}$ heterozygous embryonic kidney is shown. Note expression by both posterior Wolffian duct and metanephric mesenchyme. The broken line indicates the approximate position corresponding to the section shown in C. (C) In situ analysis on section reveals *Grem1* expression locally in the metanephric mesenchyme surrounding the ureter tips. (D) Growth of the ureter and invasion of the metanephric mesenchyme in wild-type embryos occurs by E11.25. This growth and invasion results in upregulation of *Pax2* expression in the induced mesenchyme in wild type, while it remains low in mutant mesenchyme. (E) In contrast to the wild type, *Pax2* expression is lost from mutant mesenchyme by E12.5, while it remains similar to the wild type in the Wolffian duct. (F) In contrast to the wild type, *Bmp2* fails to be expressed by the nephrogenic regions of mutant embryos. (G) In wild-type embryos, *Bmp7* expression is induced to high levels within the condensing mesenchyme. This induction is completely disrupted in *Grem1*-deficient embryos. In D-G, only the metanephric region is shown. cm, condensing metanephric mesenchyme; gr, genital ridge; mm, metanephric mesenchyme; ub, ureteric bud; ur, ureter; wd, Wolffian duct.

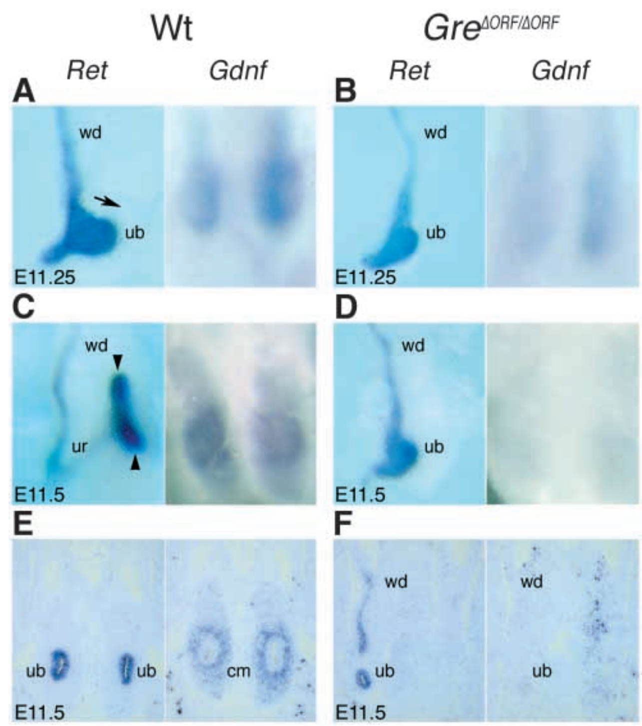

Fig. 7. Disruption of induction of ureter growth and RET/GDNF feedback signaling during metanephric organogenesis. (A) During onset of ureter growth (arrow) in wild-type embryos, *Gdnf* transcription is upregulated in the induced metanephric mesenchyme. (B) Ureter growth and *Gdnf* upregulation are not induced in mutant embryos (E11.25). (C) By E11.5, the ureter has branched once and expresses high levels of *Ret* (arrowheads) and *Gdnf* is maintained in the induced metanephric mesenchyme. (D) By contrast, ureter development is arrested and *Gdnf* expression lost in *Grem1*-deficient embryos. (E,F) Analysis of *Ret* and *Gdnf* expression on sections of E11.5 embryos confirms the disruption of RET/GDNF epithelial-mesenchymal feedback signaling in mutant embryos. cm, condensing mesenchyme; ub, ureteric bud; wd, Wolffian duct. (E,F) Transverse sections at the level of hind limb buds.

similar to newborn mice homozygous for the strongest *ld* alleles (Maas et al., 1994). Indeed, Khokha et al. (Khokha et al., 2003) reported allelism between their *Grem1* loss-of-function mutation and the ld^{J} allele as trans-heterozygous mice display limb defects at birth. We have now identified the molecular lesions in both the ld^{J} and ld^{OR} alleles and shown that they disrupt, respectively, delete the *Grem1* ORF (Zuniga et al., 2004). These rather unexpected results prompted us to re-evaluate the other *ld* alleles and the proposed function of formin in regulating *Grem1* expression in the limb bud mesenchyme (Zuniga et al., 1999) using extensive reverse genetic analysis of the two genes. These studies reveal that disruption of a cis regulatory element within formin, which is required for limb bud mesenchymal expression of *Grem1* causes the *ld* limb phenotypes (Zuniga et al., 2004). In conclusion, these studies show that the existing *ld* alleles are either complete or limb bud specific *Grem1* loss-of-function mutations and that the *ld* phenotype is not caused by disruption of the C-terminal formin domain as so far assumed (reviewed by Evangelista et al., 2003; Zeller et al., 1999).

The present study establishes that *Grem1*-mediated antagonism of BMP signaling is required for proper AER formation and function. However in *Grem1*-deficient limb buds, the expression of genes controlling dorsoventral axis formation is normal (A.Z., unpublished) and both the AER and *Fgf8* expression are induced indistinguishable form wild-type limb buds (this study). The AER and *Fgf8* expression are induced by *Wnt3*/β-*catenin* and BMP signaling activities in the ectoderm during initiation of limb bud development and establishment of dorsoventral polarity (Barrow et al., 2003; Kawakami et al., 2001; Pizette et al., 2001; Soshnikova et al., 2003). *Grem1* functions subsequently by antagonizing BMP signaling in the distal limb bud mesenchyme, which is obviously essential for progression of AER formation and establishment of multi-factorial AER signaling. In *Grem1*-deficient limb buds, enhanced mesenchymal BMP signaling blocks AER maturation and signaling at an early stage and disrupts distal limb bud morphogenesis, last but not least through apoptosis of core mesenchymal cells (see also below). These results corroborate previous studies in chicken embryos, which showed that mesenchymal BMP antagonism maintains the AER and promotes distal limb bud morphogenesis (Capdevila et al., 1999; Pizette and Niswander, 1999).

Furthermore, *Grem1*-mediated BMP antagonism has been implicated in regulating *Shh* expression through its role in establishment of the SHH/FGF4 feedback loop (Capdevila et

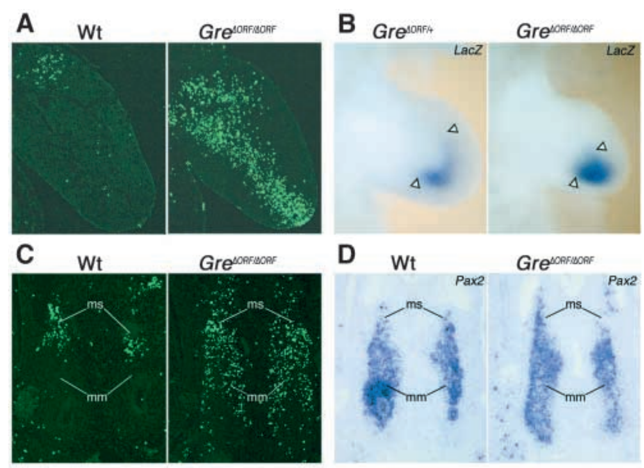

Fig. 8. *Grem1* is required for cell survival during both limb and kidney organogenesis. (A) TUNEL assay to reveal apoptotic cell death on histological sections. In the absence of *Grem1*, cells in core limb bud mesenchyme undergo massive cell death by E11.0. (B) *lacZ* transcripts are detected in E11.0 forelimb buds (whole mount) to follow the fate of cells normally expressing *Grem1* in both heterozygous and homozygous mutant limb buds. Note that *lacZ*-expressing cells survive in $Gre^{\Delta ORF/\Delta ORF}$ limb buds. White arrowheads indicate the anterior and posterior domain boundaries. Forelimb buds in A,B are shown with ventral towards the bottom and distal towards the right. (C) Massive abnormal cell death is detected by TUNEL assay in the metanephric mesenchyme (mm) of *Grem1* mutant kidneys by E11.5. Note that both wild-type and *Grem1* mutant mesonephric mesenchyme (ms) undergoes normal apoptosis at this stage. (D) *Pax2* expression in the nephrogenic tissue of a wild-type and $Gre^{\Delta ORF/\Delta ORF}$ embryo. The sections shown are adjacent to the ones shown in C. *Pax2* expression fails to be upregulated in the metanephric mesenchyme of mutant kidneys, while expression in mesonephric mesenchyme (ms) is similar to Wt. (C,D) Ventral views, posterior towards the bottom.

al., 1999; Zuniga et al., 1999; Khokha et al., 2003). During initiation of limb bud development, *Shh* expression is activated in the posterior mesenchyme under the influence of FGF8 signaling by the AER, probably in combination with FGF4 (Lewandoski et al., 2000; Moon and Capecchi, 2000; Sun et al., 2002). In particular, *Shh* is not activated in hindlimb buds lacking both *Fgf8* and *Fgf4*, despite continued expression of *Grem1* in the mesenchyme and *Fgf9*, *Fgf17* and BMP genes in the mutant AER (Sun et al., 2002). These results together with our studies (Zuniga et al., 1999) also show that *Grem1* functions initially independent of SHH in AER formation and FGF gene activation in the posterior AER**.** During progression of limb bud morphogenesis, *Grem1* induced FGF signaling by the posterior AER participates in dynamic SHH regulation as *Grem1* rescues *Shh* expression with kinetics similar to FGF4 in *ld* mutant limb buds (L.P., unpublished). The general disruption of AER-FGF signaling underlies the failure to upregulate *Shh* signaling in *Grem1*-deficient limb buds. Through establishment of feedback signaling, *Grem1* mediates the dynamic regulation of both limb bud signaling centers. For example, the distal-anterior progression of mesenchymal *Grem1* expression during limb bud morphogenesis causes anterior expansion of FGF signaling in the AER, which in turn regulates SHH signaling by the polarizing region (Zuniga et al., 1999). These dynamic changes alter the ratios of different peptide signals received by both AER cells and the underlying limb bud mesenchyme. Sanz-Ezquerro and Tickle (Sanz-Ezquerro and Tickle, 2000) have shown that the size and signaling strength of the *Shh* expression domain in limb buds is tightly regulated by apoptosis. Taken together, the analysis of epithelial-mesenchymal signaling in limb buds indicates that *Shh* expression is not regulated by a mere SHH/FGF feedback loop, but through complex and dynamic feedback signaling involving different types of mesenchyme and AER signals, and their antagonists belonging to the FGF, BMP and WNT gene families.

In *Grem1*-deficient mouse limb buds, prominent apoptotic cell death is observed in the core mesenchyme from about embryonic day 11.0 onwards. This cell death pattern is rather distinct from the ones observed in *Shh* deficient (te Welscher et al., 2002) and *Fgf4/Fgf8* double mutant (Sun et al., 2002) mouse embryos and following AER removal (Dudley et al., 2002). In addition, experiments in chicken embryos have provided evidence for a role of *Grem1*-mediated BMP antagonism in cell survival during digit formation and chondrogenesis (Merino et al., 1999). During the onset of chondrogenesis, *Grem1* acts in a paracrine fashion on the adjacent (core-) mesenchyme to protect it from undergoing programmed cell death (this study). Therefore, this anti-apoptotic function of *Grem1* could provide an explanation for the reductions and fusions of distal limb skeletal elements observed in *Grem1*-deficient mouse embryos. It is possible that the effect of *Grem1*-mediated BMP antagonism on cell survival is direct and does not involve feedback signaling between mesenchyme and AER.

The complete renal agenesis in *Grem1*-deficient mice reveals that the BMP antagonist *Grem1* is required for metanephric development. This study identifies *Grem1* as the essential extracellular signal, which initiates metanephric kidney development by enabling the ureter to invade the metanephric mesenchyme. However, establishment of the two signaling centers controlling metanephric development, the ureteric bud (expressing RET) and metanephric mesenchyme (expressing GDNF), occurs without *Grem1*; while initiation of the ureter growth and branching depend on *Grem1* function. In analogy to its function in limb buds, *Grem1* regulates the transition to dynamic signaling interactions to enable induction of metanephric organogenesis. During set-up of RET/GDNF signaling and ureteric bud formation, *Grem1* is expressed by the Wolffian duct and locally by the metanephric mesenchyme, but the primary tissue affected in *Grem1*-deficient embryos could be the ureteric epithelium as is the case in *ld* homozygous embryos (Maas et al., 1994). Such impairment of epithelium to mesenchyme signaling disrupts upregulation of *Gdnf*, *Pax2* and *Ret* expression in the mesenchyme and tips of the invading ureter, respectively. This disruption in turn leads to complete elimination of the metanephric mesenchyme by apoptotic cell death. This phenotype is strikingly similar to the one caused by inactivation of *Sall1*, a transcription factor expressed by the metanephric mesenchyme (Nishinakamura et al., 2001). However, *Sall1* remains expressed in *Grem1* mutant embryos (O.M. and A.Z., unpublished), which indicates that it is not a direct target.

Several BMP genes are expressed during initiation of metanephric kidney development and have been implicated in the early inductive events (Martinez and Bertram, 2003; Vainio and Lin, 2002). In particular, analysis of *Bmp4* heterozygous embryos has provided evidence for its essential roles during ureter morphogenesis (Miyazaki et al., 2000; Raatikainen-Ahokas et al., 2000). BMP4 (possibly similar to BMP2) (Gupta et al., 1999) inhibits ectopic branching of the ureteric bud and is required for growth of the ureter stalk. These studies (Miyazaki et al., 2000; Raatikainen-Ahokas et al., 2000), together with ours, reveal the likely mechanism by which metanephric development is initiated. Ureteric bud formation by the Wolffian duct is independent of *Grem1*-mediated BMP antagonism, while it is required to induce ureter growth, branching and propagation of RET/GDNF feedback signaling. During branching morphogenesis, *Grem1* is expressed locally in the mesenchyme surrounding the invading ureter (this study) and *Bmp4* in mesenchyme adjacent to the ureter stalk (Dudley and Robertson, 1997; Miyazaki et al., 2000). Dynamic local changes in BMP activity as mediated by antagonistic *Grem1*-BMP2/4 interactions may regulate the temporal and spatial kinetics of ureter branching, while BMP signaling alone promotes ureter stalk elongation (Miyazaki et al., 2000; Raatikainen-Ahokas et al., 2000). *Grem1*-mediated BMP4 antagonism has also been implicated in branching morphogenesis and proximodistal patterning of embryonic lungs (Lu et al., 2001; Shi et al., 2001). Consistent with these results, airway epithelia are defective in lungs of *Grem1*-deficient newborn mice (this study). In summary, the present study reveals that *Grem1*-mediated BMP antagonism regulates the dynamic interactions of diverse epithelial and mesenchymal signaling centers during progression of vertebrate organogenesis.

The authors are grateful to I. Ginez, H. Goedemans, N. Lagarde, C. Lehmann and H. Schaller for technical assistance and mouse husbandry. We thank S. Kuc for performing the *lacZ* in situ analysis; the Zentrum für Mikroskopie der Universität Basel; M. Dürrenberger and M. Düggelin for assistance with SEM analysis; and K. O'Leary for help in preparation of the manuscript. We thank S. Vainio for expert advice concerning metanephric kidney development; and F. Maina, M. Torres and S. Vainio for providing probes for in situ hybridization. We are grateful to J. Deschamps, R. Dono, A. Galli, G. Holländer, F. Meijlink, I. Mattaj and C. Torres de los Reyes for helpful discussions and comments on the manuscript. This research was supported by the Swiss National Science Foundation (to R.Z.), both cantons of Basel (to R.Z. and K.B.), the Faculty of Biology at Utrecht University, and grants from KNAW (to A.Z.) and NWO (to R.Z.).

References

Affolter, M., Bellusci, S., Itoh, N., Shilo, B., Thiery, J.-P. and Werb, Z. (2003). Tube or not tube: remodeling epithelial tissues by branching morphogenesis. *Dev. Cell* **4**, 11-18.

Avsian-Kretchmer, O. and Hsueh, A. J. (2003). Comparative genomic analysis of the eight-membered-ring cystine-knot-containing bone morphogenetic protein (BMP) antagonists. *Mol. Endocrinol*. **18**, 1-12.

Barrow, J. R., Thomas, K. R., Boussadia-Zahui, O., Moore, R., Kemler, R., Capecchi, M. R. and McMahon, A. P. (2003). Ectodermal Wnt3/beta-catenin signaling is required for the establishment and maintenance of the apical ectodermal ridge. *Genes Dev.* **17**, 394-409.

Capdevila, J., Tsukui, T., Rodriquez Esteban, C., Zappavigna, V. and Izpisua Belmonte, J. C. (1999). Control of vertebrate limb outgrowth by the proximal factor Meis2 and distal antagonism of BMPs by Gremlin. *Mol. Cell* **4**, 839-849.

Dono, R., Texido, G., Dussel, R., Ehmke, H. and Zeller, R. (1998). Impaired cerebral cortex development and blood pressure regulation in FGF-2-deficient mice. *EMBO J.* **17**, 4213-4225.

Drossopoulou, G., Lewis, K. E., Sanz-Ezquerro, J. J., Nikbakht, N., McMahon, A. P., Hofmann, C. and Tickle, C. (2000). A model for anteroposterior patterning of the vertebrate limb based on sequential long- and short-range Shh signalling and Bmp signalling. *Development* **127**, 1337-1348.

Dudley, A. T., Lyons, K. M. and Robertson, E. J. (1995). A requirement for bone morphogenetic protein-7 during development of the mammalian kidney and eye. *Genes Dev.* **9**, 2795-2807.

Dudley, A. T. and Robertson, E. J. (1997). Overlapping expression domains of bone morphogenetic protein family members potentially account for limited tissue defects in BMP7 deficient embryos. *Dev. Dyn.* **208**, 349-362.

Dudley, A. T., Ros, M. A. and Tabin, C. J. (2002). A re-examination of proximodistal patterning during vertebrate limb development. *Nature* **418**, 539-544.

Evangelista, M., Zigmond, S. and Boone, C. (2003). Formins: signaling effectors for assembly and polarization of actin filaments. *J. Cell Sci.* **116**, 2603-2611.

Gupta, I. R., Piscione, T. D., Grisaru, S., Phan, T., Macias-Silva, M., Zhou, X., Whiteside, C., Wrana, J. L. and Rosenblum, N. D. (1999). Protein kinase A is a negative regulator of renal branching morphogenesis and modulates inhibitory and stimulatory morphogenetic proteins. *J. Biol. Chem.* **274**, 26305-26314.

Haramis, A. G., Brown, J. M. and Zeller, R. (1995). The limb deformity mutation disrupts the SHH/FGF-4 feedback loop and regulation of 5′HoxD genes during limb pattern formation. *Development* **121**, 4237-4245.

Hellmich, H. L., Kos, L., Cho, E. S., Mahon, K. A. and Zimmer, A. (1996). Embryonic expression of glial cell-line derived neurotrophic factor (GDNF) suggests multiple developmental roles in neural differentiation and epithelial-mesenchymal interactions. *Mech. Dev.* **54**, 95-105.

Hsu, D., Economides, A., Wang, X., Eimon, P. and Harland, R. (1998). The Xenopus dorsalizing factor Gremlin identifies a novel family of secreted proteins that antagonize BMP activities. *Mol. Cell* **5**, 673-683.

Kawakami, Y., Capdevila, J., Buscher, D., Itoh, T., Rodriguez Esteban, C. and Izpisua Belmonte, J. C. (2001). WNT signals control FGF-dependent limb initiation and AER induction in the chick embryo. *Cell* **104**, 891-900.

Khokha, M. K., Hsu, D., Brunet, L. J., Dionne, M. S. and Harland, R. M. (2003). Gremlin is the BMP antagonist required for maintenance of Shh and Fgf signals during limb patterning. *Nat. Genet.* **34**, 303-307.

Kreidberg, J. A., Sariola, H., Loring, J. M., Maeda, M., Pelletier, J., Housman, D. and Jaenisch, R. (1993). WT-1 is required for early kidney development. *Cell* **74**, 679-691.

Lewandoski, M., Sun, X. and Martin, G. R. (2000). Fgf8 signalling from the AER is essential for normal limb development. *Nat. Genet.* **26**, 460-463.

Lu, M. M., Yang, H., Zhang, L., Shu, W., Blair, D. G. and Morrisey, E. E. (2001). The bone morphogenetic protein antagonist gremlin regulates proximal-distal patterning of the lung. *Dev. Dyn.* **222**, 667-680.

Luo, G., Hofmann, C., Bronckers, A. L., Sohocki, M., Bradley, A. and Karsenty, G. (1995). BMP-7 is an inducer of nephrogenesis, and is also required for eye development and skeletal patterning. *Genes Dev.* **9**, 2808-2820.

Maas, R., Elfering, S., Glaser, T. and Jepeal, L. (1994). Deficient outgrowth of the ureteric bud underlies the renal agenesis phenotype in mice manifesting the limb deformity (ld) mutation. *Dev. Dyn.* **199**, 214-228.

Martin, G. R. (1998). The roles of FGFs in the early development of vertebrate limbs. *Genes Dev.* **12**, 1571-1586.

Martinez, G. and Bertram, J. F. (2003). Organisation of bone morphogenetic proteins in renal development. *Nephron Exp. Nephrol.* **93**, e18-e22.

Merino, R., Rodriguez-Leon, J., Macias, D., Ganan, Y., Economides, A. N. and Hurle, J. M. (1999). The BMP antagonist Gremlin regulates outgrowth, chondrogenesis and programmed cell death in the developing limb. *Development* **126**, 5515-5522.

Miyazaki, Y., Oshima, K., Fogo, A., Hogan, B. L. and Ichikawa, I. (2000). Bone morphogenetic protein 4 regulates the budding site and elongation of the mouse ureter. *J. Clin. Invest.* **105**, 863-873.

Moon, A. M. and Capecchi, M. R. (2000). Fgf8 is required for outgrowth and patterning of the limbs. *Nat. Genet.* **26**, 455-459.

Nishinakamura, R., Matsumoto, Y., Nakao, K., Nakamura, K., Sato, A., Copeland, N. G., Gilbert, D. J., Jenkins, N. A., Scully, S., Lacey, D. L. et al. (2001). Murine homolog of SALL1 is essential for ureteric bud invasion in kidney development. *Development* **128**, 3105-3115.

Pachnis, V., Mankoo, B. and Costantini, F. (1993). Expression of the c-ret proto-oncogene during mouse embryogenesis. *Development* **119**, 1005-1017.

Panman, L. and Zeller, R. (2003). Patterning the limb before and after SHH signalling. *J. Anat.* **202**, 3-12.

Pearce, J. J., Penny, G. and Rossant, J. (1999). A mouse cerberus/Dan-related gene family. *Dev. Biol.* **209**, 98-110.

Pizette, S. and Niswander, L. (1999). BMPs negatively regulate structure and function of the limb apical ectodermal ridge. *Development* **126**, 883-894.

Pizette, S., Abate-Shen, C. and Niswander, L. (2001). BMP controls proximodistal outgrowth, via induction of the apical ectodermal ridge, and dorsoventral patterning in the vertebrate limb. *Development* **128**, 4463-4474.

Raatikainen-Ahokas, A., Hytonen, M., Tenhunen, A., Sainio, K. and Sariola, H. (2000). BMP-4 affects the differentiation of metanephric mesenchyme and reveals an early anterior-posterior axis of the embryonic kidney. *Dev. Dyn.* **217**, 146-158.

Riddle, R. D., Johnson, R. L., Laufer, E. and Tabin, C. (1993). *Sonic hedgehog* mediates the polarizing activity of the ZPA. *Cell* **75**, 1401-1416.

Sanz-Ezquerro, J. J. and Tickle, C. (2000). Autoregulation of Shh expression and Shh induction of cell death suggest a mechanism for modulating polarising activity during chick limb development. *Development* **127**, 4811-4823.

Saxén, L. (1987). *Organogenesis of the Kidney*. Cambridge, UK: Cambridge University Press.

Shi, W., Zhao, J., Anderson, K. D. and Warburton, D. (2001). Gremlin negatively modulates BMP-4 induction of embryonic mouse lung branching morphogenesis. *Am. J. Physiol. Lung Cell Mol. Physiol.* **280**, L1030-L1039.

Soshnikova, N., Zechner, D., Huelsken, J., Mishina, Y., Behringer, R. R., Taketo, M. M., Crenshaw, E. B., 3rd and Birchmeier, W. (2003). Genetic interaction between Wnt/beta-catenin and BMP receptor signaling during formation of the AER and the dorsal-ventral axis in the limb. *Genes Dev.* **17**, 1963-1968.

Sun, X., Mariani, F. V. and Martin, G. R. (2002). Functions of FGF signalling from the apical ectodermal ridge in limb development. *Nature* **418**, 501-508.

te Welscher, P., Zuniga, A., Kuijper, S., Drenth, T., Goedemans, H. J., Meijlink, F. and Zeller, R. (2002). Progression of vertebrate limb development through SHH-mediated counteraction of GLI3. *Science* **298**, 827-830.

Tickle, C. (2003). Patterning systems–from one end of the limb to the other. *Dev. Cell* **4**, 449-458.

Torres, M., Gomez-Pardo, E., Dressler, G. R. and Gruss, P. (1995). Pax-2 controls multiple steps of urogenital development. *Development* **121**, 4057-4065.

Towers, P. R., Woolf, A. S. and Hardman, P. (1998). Glial cell line-derived neurotrophic factor stimulates ureteric bud outgrowth and enhances survival of ureteric bud cells in vitro. *Exp. Nephrol.* **6**, 337-351.

Vainio, S. and Lin, Y. (2002). Coordinating early kidney development: lessons from gene targeting. *Nat. Rev. Genet.* **3**, 533-543.

Zeller, R., Haramis, A., Zuniga, A., McGuigan, C., Dono, R., Davidson, G., Chabanis, S. and Gibson, T. (1999). *Formin* defines a large family of morphoregulatory genes and functions in establishment of the polarising region. *Cell Tissue Res.* **296**, 85-93.

Zuniga, A., Haramis, A. P., McMahon, A. P. and Zeller, R. (1999). Signal relay by BMP antagonism controls the SHH/FGF4 feedback loop in vertebrate limb buds. *Nature* **401**, 598-602.

Zuniga, A., Michos, O., Spitz, F., Haramis, A. P. G., Panman, L., Galli, A., Vintersten, K., Klasen, C., Mansfield, W., Kuc, S., Duboule, D., Dono, R. and Zeller, R. (2004). Mouse *limb deformity* mutations disrupt a global control region within the large regulatory landscape required for *Gremlin* expression. *Genes Dev* (in press).